Magnetic Carbon

Nanoengineering of a Magnetically Separable Hydrogenation Catalyst**

*An-Hui Lu, Wolfgang Schmidt, Nina Matoussevitch, Helmut Bönnemann, Bernd Spliethoff, Bernd Tesche, Eckhard Bill, Wolfgang Kiefer, and Ferdi Schüth**

Mesoporous materials, with a variety of desired properties, are extensively used as absorbents, catalysts, and supports in the chemical and petrochemical industries. Very interesting members of this class of materials are ordered mesoporous carbons (OMC),[1] which are obtained by nanocasting from ordered mesoporous silica[2] as a mould. Porous carbon materials combine chemical inertness, biocompatibility, and thermal stability, and are thus suitable for many different applications. However, carbons are notoriously difficult to separate from solutions, and thus magnetic separation is an attractive alternative to filtration or centrifugation and therefore high on the wish list in catalysis for a long time.[3] Introduction of ferromagnetism in carbon particles while retaining their pore system is difficult, though: The commonly employed strategy to synthesize magnetic carbon materials is the condensation of divalent and trivalent iron salts in an activated carbon slurry in the presence of hydroxide with subsequent calcination.[4] Magnetic silica gel can be synthesized by entrapment of magnetite particles in the forming gel.[5] In the case of carbon, the resulting material has typically surface areas of around 600 $m^2 g^{-1}$ and a pore volume below 0.2 $cm^3 g^{-1}$.[4] Such synthetic procedures, however, lead to substantial blocking of the pore space, whereas the pore size distribution of the carbons is inherently broad. In addition, the materials are not stable against corrosive media or high temperature, which lead to dissolution of the magnetic component or coalescence of the particles, respectively, thus sacrificing most of the advantages of the carbon.

To overcome these limitation, we used a combination of nanocasting, spatially selective deposition of magnetic nanoparticles, protection of the nanoparticles by a nanometer-thick carbon layer,[6] and subsequent introduction of the catalytically active component to nanoengineer a magnetically separable catalyst characterized by various distinct features on the nanometer length scale. The overall synthetic strategy is shown in Scheme 1, which includes: 1) the use of

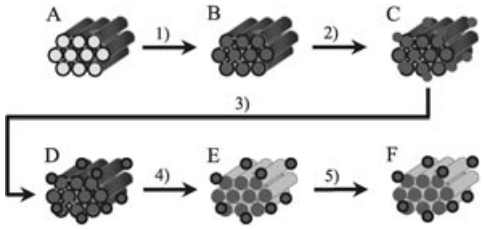

Scheme 1. Illustration of the synthesis procedure: A) ordered mesoporous silica SBA-15; B) carbon/SBA-15 composite; C) B with surface-deposited cobalt nanoparticles; D) protected cobalt nanoparticles on C; E) magnetic-ordered mesoporous carbon; F) Pd on E. 1) Carbonization of the carbon precursor in SBA-15; 2) incorporation of cobalt nanoparticles on B; 3) coating of carbon on cobalt nanoparticles; 4) dissolution of silica to create pore system; 5) loading of Pd in pores to introduce catalytic function.

the mesostructured SBA-15[2b] as template to synthesize a carbon/SBA-15 composite; 2) deposition of cobalt nanoparticles[7] selectively on the outer surface of the composite particle; 3) protection of the cobalt particles by a nanometer-thick carbon layer; 4) removal of the silica scaffold by an aqueous solution of hydrofluoric acid (HF); 5) loading the now-accessible pore system by an impregnation process with a catalytically active noble metal. A related process that involves reversible polymer protection of the pore system has been developed to produce magnetic ordered mesoporous silica.[8]

The success of this strategy can be recognized best when the material obtained after step 4 is analyzed. Transmission electron microscopy of these materials reveals the typical noodle-shaped morphology of SBA-15, which is the result of the nanocasting process (Figure 1a). The well-dispersed cobalt nanoparticles grafted on the mesoporous carbon can be clearly observed. Elemental analysis reveals a cobalt content close to the nominal amount adjusted in the impregnation step. The material, discussed in detail below, has a loading of 9 wt.%.

Higher resolution TEM analysis (Figure 1b) shows that the resulting mesoporous carbon exhibits an ordered structure with hexagonal symmetry, the typical characteristic of OMC templated from SBA-15.[9] The center-to-center distances of adjacent channels are about 7.8 nm. The cobalt particles, highly dispersed on the surface of the carbon particles, have a uniform diameter of about 11 ± 2 nm, while the original size of the cobalt nanoparticles was about 10 ± 1 nm. The increase in diameter is attributed to the coating with the carbon layer, the thickness of which roughly corresponds to three graphite layers. The formation of the carbon layer is preferentially induced on the cobalt particles as the carbonization of the furfuryl alcohol is strongly catalyzed by the cobalt. The pore system, on the other hand, remains accessible (see below). As the sample shown in

[*] Dr. A.-H. Lu, Dr. W. Schmidt, Dr. N. Matoussevitch, Prof. Dr. H. Bönnemann, B. Spliethoff, Dr. B. Tesche, Prof. Dr. F. Schüth
Max-Planck-Institut für Kohlenforschung
45470 Mülheim an der Ruhr (Germany)
Fax: (+49) 208-306-2395
E-mail: schueth@mpi-muelheim.mpg.de
Dr. E. Bill
Max-Planck-Institut für Bioanorganische Chemie
45470 Mülheim an der Ruhr (Germany)
Prof. Dr. W. Kiefer
Institut für Physikalische Chemie
Universität Würzburg
Am Hubland, 97074 Würzburg (Germany)

[**] A.-H. Lu, acknowledges the Alexander von Humboldt Foundation for a scholarship. The authors would like to thank the Leibniz-Program and the FCI for support in addition to the basic funding provided by the Institute.

 DOI: 10.1002/ange.200454222

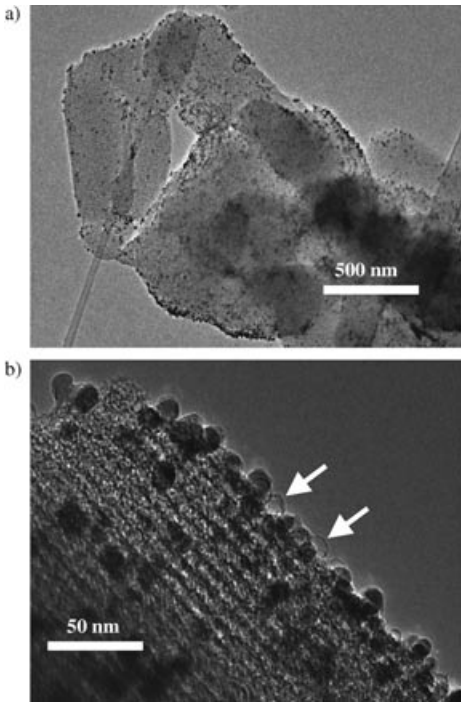

Figure 1. TEM images of Co–OMC at different magnification: a) low magnification; b) high magnification. Arrows indicate hollow carbon shells left after the leaching procedure.

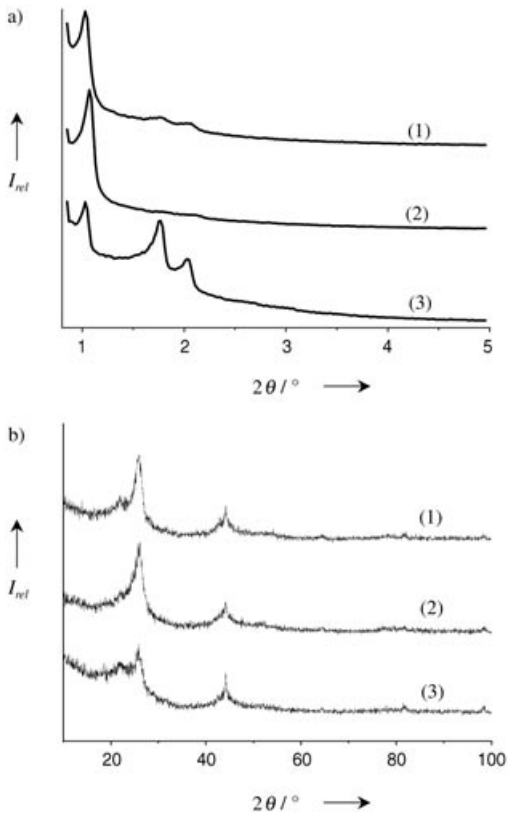

Figure 2. XRD patterns of different Co–OMC: a) low angle; b) wide angle. Types of mesoporous carbons shown in the Figure are: 1) magnetic CMK-3, 2) magnetic polyacrylonitrile-based OMC, and 3) magnetic CMK-5.

Figure 1 had been leached in HF for 72 h, one can infer that the coating of the cobalt nanoparticles is perfect in most cases and the particles are well protected against acid erosion. However, in addition to the intact particles, one can observe the existence of hollow carbon shells (arrows), which are the result of dissolution of the cobalt core by HF solution, while the imperfect shells remain. It is noteworthy that the cobalt nanoparticles do not sinter even after thermal treatment at temperatures up to 850 °C. This can be attributed to the passivation and stabilization of the cobalt nanoparticles by carbon layers through the decrease of the surface energy, and the strong interaction between the carbon coating of the cobalt particles and the bulk carbon material of the OMC.

The low-angle X-ray powder diffraction (XRD) pattern (Figure 2a) of the resultant Co–OMC shows well-resolved reflections, thus indicating an ordered structure. This is consistent with the TEM observation. The d (100) value is about 7.8 nm, from which a unit cell parameter of $a = 9.0$ nm (assuming space group *P6mm*) can be calculated, which is in reasonable agreement with the TEM analysis. The wide-angle XRD reflection (Figure 2b) matches the face-centered cubic (fcc) structure of cobalt. No indication of hexagonal close packing (hcp) cobalt was observed. The size of the cobalt particles, calculated with the Scherrer equation from the reflection broadening of the wide angle reflections, is around 10 nm, which is almost identical to the value estimated from the TEM analysis. Also shown in the Figure are the XRD patterns of two other ordered mesoporous magnetic carbons, which are either based on a different structure, that is, CMK-5,[1b,c] or on a different framework composition, that is, a carbon–nitrogen framework[10] derived from a polyacrylonitrile precursor. This observation demonstrates the general applicability of the pathway described.

The textural properties of Co–OMC were examined by nitrogen adsorption. The isotherm presented in Figure 3 is of

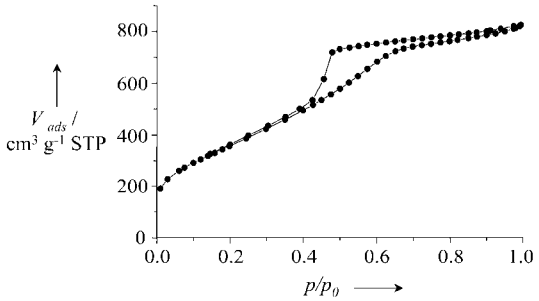

Figure 3. Nitrogen adsorption isotherm of Co–OMC.

type IV and exhibits a hysteresis loop in the relative pressure range of 0.45–0.60, thus indicating a narrow pore-size distribution in the mesopore range and proving the accessibility of the pore system. The pore-size distribution is mainly located around 3–4 nm, and the average pore size calculated by the BJH (Barrett-Joyner-Halenda) algorithm based on the adsorption branch is 3.8 nm (due to the closure of the hysteresis around $p/p_0 = 0.42$, the desorption branch was not used to avoid errors due to instability of the meniscus at this

point).[11] The actual pore size may be slightly larger, as the BJH method is known to underestimate the pore size in this range.[11] The specific surface area and pore volume are as high as 1319 $m^2 g^{-1}$ and 1.25 $cm^3 g^{-1}$, respectively, which by far exceed the textural parameters of any other magnetic material reported so far.

These data indicate one potential application of unmodified Co–OMC, that is, its use as easily recoverable adsorbent. As an example, the adsorption of the dye Rhodamine 6G (Rh6G, $C_{28}H_{31}N_2O_3Cl$) from aqueous solutions, by using Co–OMC as adsorbent, was investigated. The concentration of the Rh6G solution was 0.1 $g L^{-1}$. After the addition of Co–OMC to the Rh6G-containing solution, there was a change from orange-red to colorless within minutes, thus indicating that the Rh6G dye is strongly adsorbed by Co–OMC. The dye-loaded Co–OMC was separated by placing a conventional laboratory magnet near the glass bottle. As shown in Figure 4, the black particles were attracted to the magnet, the

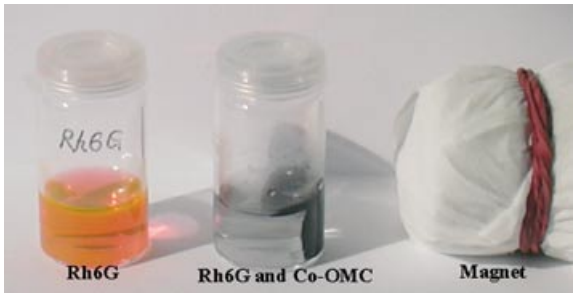

Figure 4. Rh6G aqueous solution (left) and after adsorption of the Rh6G on Co–OMC and separation of the dye loaded Co–OMC by a magnet (right).

clear solution could be decanted off or removed by pipette. This simple experiment demonstrates that the Co–OMC is magnetic and can potentially be used as a magnetic adsorbent to remove dyes or other large molecules in liquid-phase processes.

To study the magnetic properties of the materials in more detail, magnetization measurements of 9 wt.% Co–OMC were performed as a function of temperature from 2 K to 290 K in a magnetic field of $B = 1.0$ T. The magnetization (12.8 $emu g^{-1}$) of the cobalt nanoparticles is essentially temperature-independent, the effective magnetic moment increases following approximately a square-root dependence with increasing temperature. Saturation of magnetization at room temperature is reached with applied fields of about 1 T without observable hysteresis. The saturation magnetic moment (12.8 $emu g^{-1}$) corresponds to 1.5 spins per cobalt atom, which perfectly matches the value for bulk cobalt metal. This shows that the cobalt nanoparticles are in the ferromagnetic state. Oxidation would lead to the formation of antiferromagnetic spinel type oxide. The ferromagnetic properties thus demonstrate that the cobalt particles are still intact, even though this particular sample was stored under air for more than 5 months.

Magnetically separable carbon-catalyst supports are highly attractive for many applications, as carbon supports are often used in liquid-phase processes. For such applications, the particle sizes need to be small to avoid mass-transfer limitations. Small particles, however, create severe problems with respect to catalyst separation. To test the performance of the magnetic OMC as catalyst support, the hydrogenation of octene to octane was selected as a simple test reaction. Catalytic activity was introduced by loading the magnetically modified carbon with palladium. The catalyst was used as a slurry in a small, well-stirred reactor that had a continuous supply of hydrogen, and the hydrogen consumption was monitored as a measure of the progress of the reaction (Figure 5). The rate of hydrogen consumption stayed con-

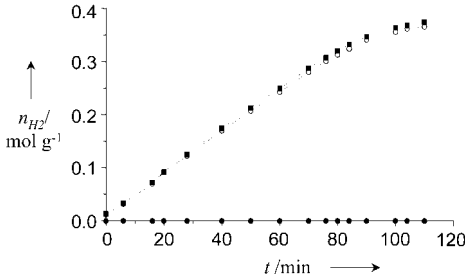

Figure 5. Hydrogenation of octene over 1% Pd-loaded Co–OMC. (■) Fist run, (○) second run after separation of catalyst and new addition of octene, (●) run to test how separable the catalyst is after magnetic removal of catalyst and readmission of hydrogen.

stant, thus indicating a continuous transformation of octene into octane until all octene had been converted. The reacted solution was removed by pipette after the magnetic carbon had been separated from the solution by applying a magnetic field to the reactor. The hydrogenation reaction was repeated by refilling fresh octene into the reactor. It was found that the reaction rate was almost identical to the initial run. This demonstrates the reproducibility of the octene hydrogenation catalyzed by Pd loaded Co–OMC.

More importantly from the point of view of an application, it is possible to remove the catalyst completely after the reaction. This aspect was checked by the following experiment: During the reaction, the catalyst was attracted to the bottom of the reactor by the application of a magnetic field. Subsequently, the partly reacted solution was transferred to a new reactor, which was once again exposed to hydrogen to carry out a new hydrogenation. However, as expected for full separation of the catalyst, no hydrogen consumption was detected. To exclude complete consumption of the octene prior to the separation, fresh octene was added. Again, no hydrogen was consumed. These experiments prove the that the catalyst can be completely separated from the reaction solution.

In summary, by using a sequence of well designed manipulation steps commonly employed in the synthesis of nanomaterials, ordered mesoporous carbons with surface-grafted magnetic particles was successfully synthesized. Such magnetic nanocomposites have very high surface area, a large pore volume, and uniform pore size. Applications of this Co–OMC as magnetically separable adsorbent and catalyst were demonstrated in this study. However, one may envisage also

other applications, such as a magnetically directed drug carrier. If a drug were loaded onto the porous carbon, one could possibly accumulate the magnetic particles in the target area of the organism, and then induce release of the drug by magnetic heating of the particles. Experiments in progress will show whether such applications can be realized.

Experimental Section

The detailed synthesis of SBA-15 can be found elsewhere.[2b] In short, tetraethyl orthosilicate (TEOS) (8.5 g, 6.9 mmol; Aldrich) were hydrolyzed at 40 °C in an aqueous solution that contained surfactant P123 (4.0 g, mol; BASF), distilled water (105 g) and aqueous 37% HCl (20 mL; Fluka). The milky mixture was aged at 90 °C for 2 days. SBA-15 was obtained after calcination at 550 °C in air. Subsequently, diluted furfuryl alcohol (Fluka) in trimethylbenzene (Fluka) was infiltrated into SBA-15 in the presence of oxalic acid as catalyst by incipient wetness impregnation with a molar ratio of furfuryl alcohol to oxalic acid of 200. The concentration of furfuryl alcohol can be varied from 30 vol.% to 80 vol.%. After the polymerization of furfuryl alcohol first at 60 °C, then at 80 °C, the carbon/SBA-15 composite was obtained by carbonization at 850 °C for 4 h under argon.[1c]

Cobalt nanoparticles were synthesized by using $[Co_2(CO)_8]$ as the source of cobalt and toluene as solvent. The nanoparticles were stabilized with the surfactant Korantin SH.[7]

The obtained carbon/SBA-15 composite was contacted with the desired amount of cobalt nanoparticles dispersed in toluene. Subsequently, toluene was removed by evacuation. To encapsulate the cobalt particles with carbon, the dried sample was impregnated with furfuryl alcohol solution followed by polymerization and carbonization up to 850 °C for 4 h. OMC with surface-grated cobalt nanoparticles was obtained by dissolving the silica in an aqueous solution of hydrofluoric acid (40%, Fluka) for 72 h.

Pd-loaded magnetic carbon was prepared by incipient wetness impregnation of Co–OMC with an aqueous solution of $Pd[(NH_3)_4Cl_2]$. The loading amount of Pd over the sample described herein was determined as 1 wt.%, but samples with higher loading were also prepared. After drying, Pd was reduced under hydrogen at 400 °C for 2 h. For the octane hydrogenation, 6 mL of octene and 0.068 g Pd-containing Co–OMC were used.

TEM images of samples were obtained with an Hitachi HF2000 microscope equipped with a cold-field emission gun. The acceleration voltage was 200 kV. Samples were prepared dry on a lacey carbon grid. Low-angle X-ray diffraction patterns of samples were recorded with a Stoe Stadi P diffractometer in the Bragg-Brentano (reflection) geometry. The step width was 0.02° at an acquisition time of 8 s per step in the range of 2θ 0.85–5°. Nitrogen-adsorption isotherms were measured with an ASAP2010 adsorption analyzer (Micromeritics) at liquid-nitrogen temperature. Magnetic susceptibility measurements were performed on a SQUID susceptometer (Quantum Design, MPMS-7) with an applied magnetic field of 0–7 T. The powdered sample was immobilized in a hard gelation capsule during the measurement. Sample temperatures were varied from 2–290 K.

Received: March 9, 2004 [Z54222]

Keywords: carbon allotropes · heterogeneous catalysis · hydrogenation · magnetic carbon · mesoporous compounds

[1] a) R. Ryoo, S. H. Joo, S. Jun, *J. Phys. Chem. B* **1999**, *103*, 7743–7746; b) S. H. Joo, S. J. Choi, I. Oh, J. Kwak, Z. Liu, O. Terasaki, R. Ryoo, *Nature* **2001**, *412*, 169–172; c) A.-H. Lu, W. Li, W. Schmidt, W. Kiefer, F. Schüth, *Carbon*, accepted.

[2] a) C. T. Kresge, M. E. Leonowicz, W. J. Roth, J. C. Vartuli, J. S. Beck, *Nature* **1992**, *359*, 710–712; b) D. Zhao, J. Feng, Q. Huo, N. Melosh, G. H. Fredrickson, B. F. Chmelka, G. D. Stucky, *Science* **1998**, *279*, 548–552.

[3] W. Teunissen, F. M. F. de Groot, J. Geus, O. Stephan, M. Tence, C. Colliex, *J. Catal.* **2001**, *204*, 169–174.

[4] L. C. A. Olivera, R. V. R. A. Rios, J. D. Fabris, V. Garg, K. Sapag, R. M. Lago, *Carbon* **2002**, *40*, 2177–2183.

[5] M. T. Reetz, A. Zonta, V. Vijayakrishnan, K. Schimossek, *J. Mol. Catal. A* **998**, *134*, 251–258.

[6] R. S. Ruoff, D. C. Lorents, B. Chan, R. Malhotra, S. Subramoney, *Science* **1993**, *259*, 346–348.

[7] H. Bönnemann, W. Brijoux, R. Brinkmann, N. Matoussevitch, N. Waldöfner, N. Palina, H. Modrow, *Inorg. Chim. Act*a. **2003**, *350*, 617–624.

[8] A.-H- Lu, W. Li, A. Kiefer, W. Schmidt, E. Bill, G. Fink, F. Schüth, *J. Am. Chem. Soc.*, **2004**, *126*, 8616.

[9] R. Ryoo, S. H. Joo, M. Kruk, M. Jaroniec, *Adv. Mater.* **2001**, *13*, 677–681.

[10] A.-H. Lu, A. Kiefer, W. Schmidt, F. Schüth, *Chem. Mater.* **2004**, *16*, 100–103.

[11] M. Kruk, M. Jaroniec, *Chem. Mater.* **2001**, *13*, 3169–3183.

